Sequential Co-Design of an Artifact and its Controller Via Control Proxy Functions

Diane L. Peters * **Panos Y. Papalambros** ** **A. Galip Ulsoy** ***

* *Mechanical Engineering Department, University of Michigan, Ann Arbor, MI 48109 USA (e-mail: dlpeters@umich.edu).*
** *Mechanical Engineering Department, University of Michigan, Ann Arbor, MI 48109 USA (e-mail: pyp@umich.edu)*
*** *Mechanical Engineering Department, University of Michigan, Ann Arbor, MI 48109 USA (e-mail: ulsoy@umich.edu)*

Abstract: Optimization of a 'smart' product requires optimizing the design of both the artifact and its controller. If the artifact and control optimization are coupled, then a combined approach is typically used in order to produce optimal solutions. The combined approach presents certain disadvantages, however. In particular, it precludes the decomposition of the problem into smaller functional sub-problems, and requires the formulation of both the artifact and control objectives and constraints before solving either optimization problem. In this paper, it is shown that a modified sequential approach utilizing a Control Proxy Function (CPF) can be used to produce optimal, or near-optimal, solutions while allowing this decomposition. Two physical bases for CPFs are presented, natural frequency and the controllability Grammian matrix, and their range of applicability is discussed. These concepts are demonstrated on a positioning gantry example.

Keywords: co-design, design optimization, controller design

1. INTRODUCTION

The design of many systems requires both the design of the physical system, or artifact, and a controller. In the optimal design and control of such 'smart' systems, both an artifact objective function, f_a, and a control objective function, f_c, may be formulated, subject to artifact inequality and equality constraints, $\boldsymbol{g_a}$ and $\boldsymbol{h_a}$, and control inequality and equality constraints, $\boldsymbol{g_c}$ and $\boldsymbol{h_c}$. These objectives and constraints are functions of artifact and controller design variables, denoted as $\boldsymbol{d_a}$ and $\boldsymbol{d_c}$, respectively. In the most general case, all of the objectives and constraints may be functions of both sets of variables, i.e., $f_a = f_a(\boldsymbol{d_a}, \boldsymbol{d_c})$, $\boldsymbol{g_a} = \boldsymbol{g_a}(\boldsymbol{d_a}, \boldsymbol{d_c})$, $\boldsymbol{h_a} = \boldsymbol{h_a}(\boldsymbol{d_a}, \boldsymbol{d_c})$, $f_c = f_c(\boldsymbol{d_a}, \boldsymbol{d_c})$, $\boldsymbol{g_c} = \boldsymbol{g_c}(\boldsymbol{d_a}, \boldsymbol{d_c})$, and $\boldsymbol{h_c} = \boldsymbol{h_c}(\boldsymbol{d_a}, \boldsymbol{d_c})$. This optimal design and control problem, denoted as co-design, can present special challenges when the design of the artifact and controller are dependent on one another. In this situation, the solution of the bi-objective co-design problem given by Eqs.(1) - (5) is a Pareto set, with the various Pareto points found by varying the weights w_a and w_c, and the problem is said to be coupled.

$$\min_{\boldsymbol{d_a}, \boldsymbol{d_c}} \quad w_a f_a + w_c f_c \tag{1}$$

$$\text{subject to} \quad \boldsymbol{g_a} \leq \boldsymbol{0} \tag{2}$$

$$\boldsymbol{h_a} = \boldsymbol{0} \tag{3}$$

$$\boldsymbol{g_c} \leq \boldsymbol{0} \tag{4}$$

$$\boldsymbol{h_c} = \boldsymbol{0} \tag{5}$$

When all of the objective and constraint functions depend on both $\boldsymbol{d_a}$ and $\boldsymbol{d_c}$, coupling is said to be bi-directional. However, there is a large class of problems in which neither the artifact objective function nor the artifact constraints are functions of $\boldsymbol{d_c}$, i.e., $f_a = f_a(\boldsymbol{d_a})$, $\boldsymbol{g_a} = \boldsymbol{g_a}(\boldsymbol{d_a})$, and $\boldsymbol{h_a} = \boldsymbol{h_a}(\boldsymbol{d_a})$. These problems are said to exhibit uni-directional coupling. The problems considered in this work exhibit uni-directional coupling.

A variety of measures have been proposed to quantify the strength of coupling [Haftka et al. (1986); Bloebaum (1995); Fathy et al. (2004); Alyaqout et al. (2005)]. These measures have been shown to be related, though in most cases they are not commensurate with one another [Peters et al. (2009); Peters (2010)]. In problems with uni-directional coupling, one measure which is particularly useful is the coupling vector, $\boldsymbol{\Gamma_v}$, which is defined as follows [Fathy et al. (2004)].

$$\boldsymbol{\Gamma_v} = \frac{w_c}{w_a}\left(\frac{\partial f_c}{\partial \boldsymbol{d_a}} + \frac{\partial f_c}{\partial \boldsymbol{d_c}}\frac{d\boldsymbol{d_c}}{d\boldsymbol{d_a}}\right) \tag{6}$$

This vector is valid only at an optimal solution; however, at a point not known to be optimal, an estimate can be computed. The equation for the estimated coupling vector, denoted as $\hat{\boldsymbol{\Gamma}}_{\boldsymbol{v}}$, is identical to Eq. (6), but does not require the solution of Eqs. (1) - (5).

Coupled systems reported in the literature are in diverse areas including structural systems with active control [e.g., Haftka et al. (1986); Rao and Pan (1990)], micro-electrical mechanical systems, or MEMS [e.g., Carley et al. (2001); Oldham et al. (2005)], and robotics and mechatronics [e.g., Ravichandran et al. (2006); Zhu et al. (2001)]. In robotic applications, typical objectives for the artifact design are minimizing weight or minimizing deflection. Controller objectives may be minimizing tracking errors for a particular trajectory, overshoot, or settling time [Ouyang et al. (2002)]. In these problems, speed and accuracy are in conflict; mechanisms with lower inertia are more flexible, resulting in a fast response but lower accuracy, while a higher inertia will produce a stiffer mechanism that is more accurate but results in lower speeds [Zhu et al. (2001)]. Many applications, however, require both high speed and high accuracy. Therefore, design of such systems must consider the coupling between the artifact and control objectives [Park and Asada (1992)].

It has been shown that a simple sequential optimization, in which the artifact is first optimized and then the optimal control is found for that artifact, does not find the optimum for the system. Combined optimization methods such as a simultaneous strategy, in which both the artifact and control are optimized together, will produce system-optimal solutions. However, they present disadvantages. In addition to the computational complexity of the larger problem, they require the use of more than one discipline to formulate the full problem. This presents organizational challenges, since expertise in the various disciplines typically resides in different individuals, and often in different groups within an organization. Furthermore, specialized techniques developed for optimal control can no longer be used when the problem is not formulated as a purely optimal control problem.

This paper shows, for the first time, that the use of a Control Proxy Function (CPF) can provide optimal, or near-optimal, solutions to the co-design problem without the disadvantages seen in the combined optimization techniques, and that is the focus of this paper.

2. OPTIMIZATION OF COUPLED SYSTEMS USING A CONTROL PROXY FUNCTION (CPF)

In order to preserve the functional decomposition of the co-design problem while realizing optimal or near-optimal solutions, a modified sequential optimization strategy is proposed. In this strategy, the original artifact objective function, f_a, is augmented with a Control Proxy Function (CPF), representing the system's ease of control, as shown in Fig. 1. The CPF, denoted as χ, is a function only of the artifact design variables, $\boldsymbol{d_a}$. The optimization problem is then formulated as follows:

$$\min_{\boldsymbol{d_a}} \; f'_a\left(\boldsymbol{d_a}\right) = w_1 f_a\left(\boldsymbol{d_a}\right) + w_2 \chi\left(\boldsymbol{d_a}\right) \tag{7}$$

$$\text{subject to} \quad \boldsymbol{g_a}\left(\boldsymbol{d_a}\right) \leq \boldsymbol{0} \tag{8}$$

$$\boldsymbol{h_a}\left(\boldsymbol{d_a}\right) = \boldsymbol{0} \tag{9}$$

where w_1 and w_2 are positive weights representing the relative importance of the artifact objective and the CPF, followed by the control design problem

$$\min_{\boldsymbol{d_c}} \; f_c\left(\boldsymbol{d_a^*}, \boldsymbol{d_c}\right) \tag{10}$$

$$\text{subject to} \quad \boldsymbol{g_c}\left(\boldsymbol{d_a^*}, \boldsymbol{d_c}\right) \leq \boldsymbol{0} \tag{11}$$

$$\boldsymbol{h_c}\left(\boldsymbol{d_a^*}, \boldsymbol{d_c}\right) = \boldsymbol{0} \tag{12}$$

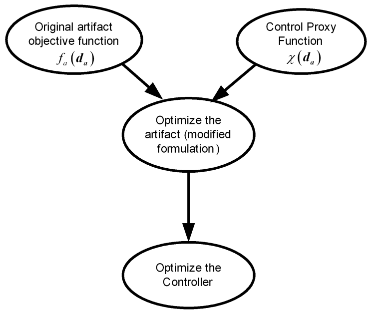

Fig. 1. Control Proxy Function Problem Formulation

where $\boldsymbol{d_a^*} = \text{argmin } f'_a\left(\boldsymbol{d_a}\right)$.

The success of the method depends on the selection of an appropriate CPF. A well-chosen CPF, which effectively captures the fundamental physical limitations of the system, will result in solutions that are close to the Pareto optimal points found by a simultaneous formulation, while a poorly chosen CPF will yield solutions far from system optimality.

The mathematical characteristics of an effective CPF have been studied, and four theorems describing appropriate CPFs have been proven [Peters (2010)]. These theorems are summarized here as follows:

(1) If $\boldsymbol{\Gamma_v}$ is parallel to $\nabla\chi$ at all points, then the CPF solution set will coincide with the Pareto frontier. A CPF satisfying this condition is said to be perfect.
(2) CPF solution points will approach the Pareto frontier as ξ, the angle between the estimate of the coupling vector $\hat{\boldsymbol{\Gamma}}_{\boldsymbol{v}}$ and $\nabla\chi$ in the $\boldsymbol{d_a}$-space, approaches zero; i.e., CPF solution points will be close to the Pareto frontier when the angle ξ is small.
(3) If the control objective function, $f_c\left(\boldsymbol{d_a}, \boldsymbol{d_c}\right)$, is monotonic with respect to some element of $\boldsymbol{d_a}$, then an effective CPF, $\chi\left(\boldsymbol{d_a}\right)$, will have the same coordinate-wise monotonicity as f_c with respect to that element of $\boldsymbol{d_a}$.
(4) If the control objective function, $f_c\left(\boldsymbol{d_a}, \boldsymbol{d_c}\right)$, has an unconstrained minimum in the $\boldsymbol{d_a}$-space, then an effective CPF, $\chi\left(\boldsymbol{d_a}\right)$, will obtain its minimum close to it.

In this paper, Theorem (1) will be particularly useful, as it can be used to determine under what conditions the particular CPFs considered will produce optimal solutions. Theorem (2) will be used to evaluate the solutions when the CPF method is applied to an example problem.

3. CONTROL PROXY FUNCTIONS FOR SPECIFIC PROBLEM FORMULATIONS

Given the characteristics of effective CPFs, we can formulate potential CPFs for specific problems and evaluate them. These specific CPFs are based on physically meaningful system characteristics, specifically the natural frequency of the system and the controllability Grammian matrix. The natural frequency is considered as the basis for a CPF because previous work has shown that, in some cases, it can be used as an effective proxy for a system's ease of control [e.g., Peters et al. (2008); Hale et al. (1985);

Khot and Abhyankar (1993)]. The controllability Grammian matrix, $\boldsymbol{W_c}$, will be considered as the basis for a CPF because it has been successfully used for the location of actuators [e.g., Muller and Weber (1972); Roh and Park (1997); Lim and Gawronski (1993)]. Furthermore, it has been shown that, for some problem formulations, there is a relationship between $\boldsymbol{W_c}$ and the coupling vector $\boldsymbol{\Gamma_v}$ [Peters et al. (2010)]. Since there is also a relationship between $\boldsymbol{\Gamma_v}$ and an effective CPF, as outlined above, this suggests that a CPF based on $\boldsymbol{W_c}$ will be perfect for some problems.

3.1 Control Proxy Function Utilizing Natural Frequency

The natural frequency has been successfully used to predispose a system to effective control, suggesting that it can be used to formulate an effective control proxy function in some cases. Naturally, the question arises what those cases might be, and how they can be identified. Here, three specific problem formulations are presented, derived in [Peters (2010)], in which natural frequency can be used in a perfect CPF. Those system characteristics that are common to all three problems are:

(1) The co-design problem is formulated as in Eq. (1)-(5), and exhibits uni-directional coupling.

(2) The system is linear and dominated by second-order dynamics. This system can be described, then, in the form

$$m\ddot{z} + b\dot{z} + kz = u(t) \tag{13}$$

where m, b, and k are functions of the design variables d_a, parameters, and constants, z is the system output, and $u(t)$ is the forcing function; or alternatively in state-space form as

$$\dot{\boldsymbol{x}} = \boldsymbol{A}\boldsymbol{x} + \boldsymbol{B}u \tag{14}$$

where

$$\boldsymbol{A} = \begin{bmatrix} 0 & 1 \\ -\dfrac{k}{m} & -\dfrac{b}{m} \end{bmatrix} \tag{15}$$

$$\boldsymbol{B} = \begin{bmatrix} 0 \\ \dfrac{1}{m} \end{bmatrix} \tag{16}$$

$$\boldsymbol{x} = \begin{bmatrix} z \\ \dot{z} \end{bmatrix} \tag{17}$$

The open-loop system is underdamped, i.e., the open-loop eigenvalues are complex.

(3) The matrix $\boldsymbol{B}$ is independent of the artifact design variables $\boldsymbol{d_a}$, i.e.,

$$\frac{\partial m}{\partial \boldsymbol{d_a}} = \boldsymbol{0}. \tag{18}$$

(4) A state-feedback controller with gains $\boldsymbol{K}$, possibly with a precompensator G, is applied to the system, as shown in Fig. 2.

(5) There are no active controller equality constraints $\boldsymbol{h_c}(\boldsymbol{d_a}, \boldsymbol{d_c})$ or strongly active controller inequality constraints $\boldsymbol{g_c}(\boldsymbol{d_a}, \boldsymbol{d_c})$ present. Weakly active controller inequality constraints may be present, where a weakly active constraint is one which is not satisfied as a strict equality but whose removal will affect the system optimum [Pomrehn and Papalambros (1994)].

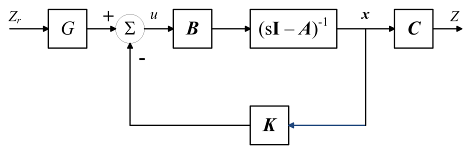

Fig. 2. Schematic of System Controller

In a second-order system, there are two eigenvalues, which are complex conjugates. These eigenvalues can be fully described by the frequency ω and damping coefficient ζ of the system.

$$\lambda_{1,2} = -\zeta\omega \pm \omega\sqrt{\zeta^2 - 1} \tag{19}$$

The natural frequency of the open-loop system will be denoted as ω_n and the damping coefficient of the open-loop system as ζ_n. The frequency of the controlled, or closed-loop, system will be denoted as ω_c and the damping coefficient of the closed-loop system will be denoted as ζ_c. The open-loop and closed-loop frequencies and damping coefficients for the second-order system subjected to state-feedback control are given by the following equations [Franklin et al. (1994)]:

$$\omega_n = \sqrt{\frac{k}{m}} \tag{20}$$

$$\zeta_n = \frac{b}{2\sqrt{mk}} \tag{21}$$

$$\omega_c = \sqrt{\frac{k + K_1}{m}} \tag{22}$$

$$\zeta_c = \frac{b + K_2}{2\sqrt{m\,(k + K_1)}} \tag{23}$$

These equations will be used to define three specific problem formulations where $\chi(\boldsymbol{d_a}) = \chi(\omega_n)$ is a perfect CPF. In each case, additional necessary conditions are specified, relating to the damping of the system.

Control Objective Independent of Damping: If the control objective f_c is a function of the closed-loop frequency ω_c of the system but is independent of the closed-loop damping coefficient ζ_c, then the CPF $\chi = \chi(\omega_n)$ will yield system-optimal solutions to the simultaneous optimization problem. An example of this control objective is $f_c = t_r$, where $t_r = \dfrac{1.8}{\omega_c}$ is the rise time of the system [Franklin et al. (1994)]. For a second-order system, ω_n is given by Eq. (20), and therefore the gradient of χ is given by

$$\nabla\chi = \frac{\partial\chi}{\partial\omega_n}\frac{\partial\omega_n}{\partial\boldsymbol{d_a}} = \frac{\partial\chi}{\partial\omega_n}\left(\frac{1}{2}\sqrt{\frac{1}{km}}\frac{\partial k}{\partial\boldsymbol{d_a}}\right) \tag{24}$$

where k is a function of $\boldsymbol{d_a}$. The closed-loop frequency of the system is given by Eq. (22). Using Eq. (6), the coupling is found to be

$$\boldsymbol{\Gamma_v} = \frac{w_2}{w_1}\frac{\partial f_c}{\partial\omega_c}\left(\frac{1}{2}\sqrt{\frac{1}{(k + K_1)\,m}}\frac{\partial k}{\partial\boldsymbol{d_a}}\right) \tag{25}$$

If the CPF is perfect, the vector computed is the coupling vector $\boldsymbol{\Gamma_v}$, not the estimate $\hat{\boldsymbol{\Gamma}}_{\boldsymbol{v}}$. It is possible, then, to express the coupling vector $\boldsymbol{\Gamma_v}$ at the CPF solution as

$$\mathbf{\Gamma}_{\boldsymbol{v}} = \frac{w_2}{w_1}\sqrt{\frac{k}{k+K_1}}\left(\frac{\partial f_c}{\partial \omega_c}\right)/\left(\frac{\partial \chi}{\partial \omega_n}\right)\nabla\chi \qquad (26)$$

and it can be seen that the coupling vector at the CPF point is equal to a scalar quantity multiplied by the gradient of the CPF. From Theorem 1, then, the CPF points will be Pareto optimal for the co-design problem.

Control Objective Independent of Imaginary Component of Eigenvalues: If the control objective f_c is a function of the product $\omega_c\zeta_c$, i.e., of the real part of the closed-loop eigenvalues (e.g., $f_c = t_s$, where t_s is the settling time of the system), and the damping ratio ζ_n of the open-loop system is independent of $\boldsymbol{d_a}$, then the CPF $\chi = \chi(\omega_n)$ will yield system-optimal solutions to the simultaneous optimization problem.

A similar procedure to that given above [Peters (2010)] can be used to derive a relationship between the coupling vector and the gradient $\nabla\chi$. This relationship is found to be

$$\mathbf{\Gamma}_{\boldsymbol{v}} = \frac{w_2}{w_1}\frac{\partial f_c}{\partial(\omega_c\zeta_c)}\frac{b}{2\sqrt{km}}\left(1/\frac{\partial \chi}{\partial \omega_n}\right)\nabla\chi \qquad (27)$$

Again, if the CPF is perfect, the vector computed is the coupling vector $\mathbf{\Gamma}_{\boldsymbol{v}}$, not the estimate $\hat{\mathbf{\Gamma}}_{\boldsymbol{v}}$. It can then be seen that the coupling vector at the CPF point is equal to a scalar multiplied by $\nabla\chi$, where $\nabla\chi$ is given by Eq. (24). Therefore, from Theorem 1, the CPF points will be Pareto optimal for the co-design problem.

Damping Term b Independent of $\boldsymbol{d_a}$: If the controller objective f_c is an arbitrary function of the closed-loop eigenvalues of the system, and the damping term b in the system description is independent of $\boldsymbol{d_a}$, i.e.,

$$\frac{\partial b}{\partial \boldsymbol{d_a}} = \mathbf{0} \qquad (28)$$

then the CPF $\chi = \chi(\omega_n)$ will yield system-optimal solutions to the simultaneous optimization problem.

Yet again, as shown in [Peters (2010)], a relationship can be derived between the coupling vector and the gradient $\nabla\chi$. This relationship is found to be

$$\mathbf{\Gamma}_{\boldsymbol{v}} = \frac{w_2}{w_1}\sqrt{\frac{k}{k+K_1}}\left(\frac{\partial f_c}{\partial \omega_c} - \frac{\partial f_c}{\partial \zeta_c}\frac{b+K_2}{2(k+K_1)}\right)\left(1/\frac{\partial \chi}{\partial \omega_n}\right)\nabla\chi \qquad (29)$$

Again, if the CPF is perfect, the vector computed is the coupling vector $\mathbf{\Gamma}_{\boldsymbol{v}}$, not the estimate $\hat{\mathbf{\Gamma}}_{\boldsymbol{v}}$. It can be seen that the coupling vector at the CPF point is equal to a scalar multiplied by $\nabla\chi$, where $\nabla\chi$ is given by Eq. (24). Therefore, from Theorem 1, the CPF points will be Pareto optimal for the co-design problem.

3.2 Control Proxy Function Utilizing the Controllability Grammian Matrix

A CPF using open-loop eigenvalues will not be effective when the matrix $\boldsymbol{B}$ is sensitive to the artifact design variables $\boldsymbol{d_a}$, since open-loop eigenvalues cannot be used to model that system behavior. For problems of this type, the CPF must be based on some other fundamental metric of the system which is capable of modeling both the free and forced response characteristics of the system. Since the controllability Grammian matrix $\boldsymbol{W_c}$ incorporates both the free and forced response characteristics of a system, it is logical to consider its use in a CPF. Here, we will demonstrate that the controllability Grammian can be used to formulate a CPF in some cases. Additional cases in which the controllability Grammian can be used are given in [Peters (2010)].

In the development of the CPF based on the controllability Grammian, it is assumed that the system dynamics are linear and time-invariant, and can be described in state-space form, i.e., by Eq. (14). The system may be of arbitrarily high order. For this system, the controllability Grammian matrix is given by [Skogestad and Postlethwaite (2005)]

$$\boldsymbol{W_c}(t_f) = \int_0^{t_f} e^{\boldsymbol{A}t}\boldsymbol{B}\boldsymbol{B}^T e^{\boldsymbol{A}^T t}dt \qquad (30)$$

The CPF that will be considered is:

$$\chi = \boldsymbol{x_f}^T\boldsymbol{W_c}^{-1}(t_f)\,\boldsymbol{x_f} \qquad (31)$$

where $\boldsymbol{x_f}$ is the final state of the system, and t_f is the time at which it reaches that state.

Control Effort as Control Objective Function: The CPF given by Eq. (31) will produce optimal solutions when the control objective function, f_c, is the control effort necessary to move the system from its zero state to its final state, $\boldsymbol{x_f}$, at a specified final time, t_f, where t_f is a parameter. The final state, $\boldsymbol{x_f}$, may be a parameter or it can be a function of the artifact design variables, $\boldsymbol{d_a}$. An example would be a positioning device in an automated assembly system; parts to be assembled typically must be placed at their destination at a particular time.

The objective function, f_c, is given by

$$f_c = \int_0^{t_f}(u(t))^2\,dt. \qquad (32)$$

The controllability Grammian matrix can be used to construct a lower bounding function for the control effort, which is given by [Skogestad and Postlethwaite (2005)]

$$f_c \geq \boldsymbol{x_f}^T\boldsymbol{W_c}^{-1}(t_f)\,\boldsymbol{x_f} \qquad (33)$$

If an optimal controller is used, then the optimal value of f_c is given by

$$f_c^* = \boldsymbol{x_f}^T\boldsymbol{W_c}^{-1}(t_f)\,\boldsymbol{x_f}, \qquad (34)$$

and it is evident that the solutions found using this CPF will be optimal since $\chi = f_c$. Furthermore, it has been shown that, for this problem,

$$\mathbf{\Gamma}_{\boldsymbol{v}} = \frac{w_c}{w_a}\frac{\partial}{\partial \boldsymbol{d_a}}\left(\boldsymbol{x_f}^T\boldsymbol{W_c}^{-1}(t_f)\,\boldsymbol{x_f}\right), \qquad (35)$$

and thus Theorem (1) confirms that the CPF given in Eq. (31) will produce optimal solutions.

Time as Control Objective Function and Control Effort as Constraint: The CPF given by Eq. (31) will produce optimal solutions when the control objective function is the time, t_f, necessary to move the system from its zero state to a final state, $\boldsymbol{x_f}$, subject to a limit on the available control energy, E_{max}, where E_{max} is a parameter. Again, $\boldsymbol{x_f}$ may be a parameter or a function of $\boldsymbol{d_a}$.

The objective function, f_c, and constraint, g_c, are given by

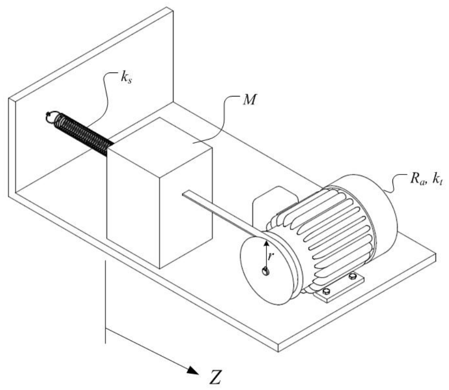

Fig. 3. Configuration of Positioning Gantry System

$$f_c = t_f \tag{36}$$

$$g_c = \int_0^{t_f} (u(t))^2 \, dt - E_{max} \leq 0 \tag{37}$$

The coupling vector for this problem is parallel to that for the problem where control effort is the objective function. Therefore, the coupling vector for this problem will also be parallel to $\nabla\chi$, where χ is given by Eq. (31). Using Theorem (1), it can be seen that the use of this CPF will result in optimal solutions.

4. ILLUSTRATIVE EXAMPLE: POSITIONING GANTRY SYSTEM

4.1 Configuration of Positioning Gantry

Consider the system shown in Fig. 3, representing a simple model of a positioning gantry. In this system, a mass M is connected to a fixed surface by a linear spring with constant k_s. A flexible belt connects to the mass and wraps around a pulley with radius r, which is mounted on a DC motor with armature resistance R_a and motor constant k_t. The displacement of the mass from its original position is Z. The system can be modeled in the form of Eqs. (13) - (17), where $m = \frac{MrR_a}{k_t}$, $b = \frac{k_t}{r}$, and $k = \frac{k_s r R_a}{k_t}$. A state-feedback controller with gains $\boldsymbol{K} = [K_1 \;\; K_2]$ and precompensator G is applied to the system, as shown in Fig. 2, to generate the input voltage u to the motor. The steady-state voltage is denoted as u_{ss}. Values of parameters are given $R_a = 2$ kΩ, $M = 2$ kg, and $u_{ss} = 10$ V.

4.2 Optimization Problem Formulation

The following objectives and constraints are selected:

$$f_a(k_t, r, k_s) = -Z_f \tag{38}$$

subject to simple bounds on the artifact design variables:

$$2.5 \leq r \leq 7.5 \tag{39}$$

$$5 \leq k_t \leq 20 \tag{40}$$

$$0.5 \leq k_s \leq 2.0 \tag{41}$$

where the final displacement Z_f represents the peak displacement, with a 10% overshoot over the steady-state displacement, Z_{ss}.

$$Z_f = 1.1 Z_{ss} = \frac{1.1 u_{ss} k_t}{r R_a k_s} \tag{42}$$

The controller objective is

$$f_c(k_t, r, k_s, K_1, K_2, G) = \int_0^{t_f} (u(t))^2 \, dt \tag{43}$$

The optimization problem is formulated as in Eqs. (7)-(12), using the CPF given by Eq. (31), where $\boldsymbol{x_f} = \begin{bmatrix} Z_f \\ 0 \end{bmatrix}$. Since this problem satisfies the conditions set on the derivation of this CPF in Section 3, it is expected that the solutions found will be system-optimal.

4.3 Optimization Results

This problem was solved using Matlab's *fmincon* function for a variety of weights w_1 and w_2, producing the results shown in Fig. 4. For each point, $\nabla\chi$ and $\hat{\boldsymbol{\Gamma}}_{\boldsymbol{v}}$ were calculated. Using these vectors, the angle ξ was calculated, and it was found that $\xi = 0$ for all points. Thus, based on Theorem (2), it is known that these solutions are system-optimal. Note that this was determined without the need to solve the simultaneous problem in Eqs. (1) - (5).

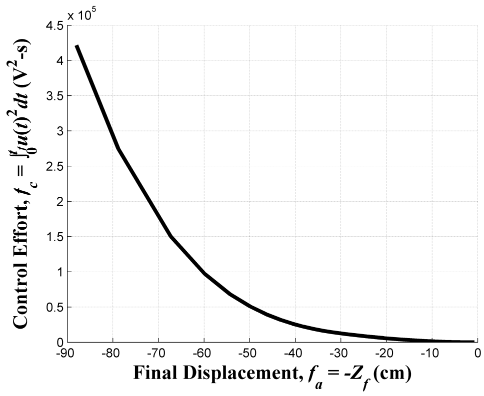

Fig. 4. Results of Positioning Gantry Optimization

5. CONCLUDING REMARKS

In this paper, a new method of solution for co-design problems, based upon a sequential optimization using a Control Proxy Function (CPF) is presented. The intent of the CPF method is to provide solutions that are identical with, or close to, the Pareto optimal solutions to the co-design problem, while allowing the problem to be decomposed into an artifact design problem and a control design problem. This decomposition allows the co-design problem to be more easily formulated and solved by experts in each of the functional areas of artifact design and control design. The key to the effectiveness of this method is the choice of an appropriate CPF, and we have proposed appropriate CPFs for specific problem formulations. These CPFs are based on the system's natural frequency and on the controllability Grammian matrix. In the case of both CPFs, we have assumed that the system of interest is linear and time-invariant. For a CPF based on natural frequency, the system was also assumed to be second-order, though the CPF based on the controllability Grammian applies to systems of arbitrarily high order. One of these CPFs, based on the controllability Grammian, was used in the optimization of a simple positioning gantry and its controller, and was shown to provide optimal solutions.

These CPFs are not exhaustive; it is possible to formulate and evaluate additional CPFs, based on open-loop eigenvalues, the controllability Grammian, and possibly other system metrics, and the development of such CPFs should be the subject of future work. These CPFs could be used to produce optimal solutions for a variety of problems not considered here, such as Linear Quadratic Gaussian (LQG) control, vehicle steering applications, trajectory control, sensor placement, and power management. In some cases, it may not be possible to develop a simple CPF that provides optimal results. However, one can conjecture that a CPF based on the controllability and observability Grammians will produce results that are near-optimal for a variety of problems, since they provide measures of how easily a system is controlled and how easily the states are estimated. This conjecture should also be investigated in future work, and it should be determined how effective a CPF based on the controllability and observability Grammians will be for various types of co-design problems.

ACKNOWLEDGEMENTS

This work was partially supported by NSF grant #0625060 and by the Automotive Research Center (ARC). This support is gratefully acknowledged.

REFERENCES

Alyaqout, S.F., Papalambros, P.Y., and Ulsoy, A.G. (2005). Quantification and use of system coupling in decomposed design optimization problems. In *Proceedings of the ASME IMECE 2005*, 95–103. ASME, Orlando, FL. Paper number IMECE2005-81364.

Bloebaum, C. (1995). Coupling strength-based system reduction for complex engineering design. *Structural Optimization*, 10, 113–121.

Carley, L., Ganger, G., Guillou, D., and Nagle, D. (2001). System design considerations for MEMS-actuated magnetic-probe-based mass storage. *IEEE Transactions on Magnetics*, 37, 657–662.

Fathy, H., Papalambros, P.Y., and Ulsoy, A.G. (2004). On combined plant and control optimization. In *8th Cairo University International Conference on Mechanical Design and Production*. Cairo University, Cairo, Egypt.

Franklin, G., Powell, J., and Emami-Naeini, A. (1994). *Feedback Control of Dynamic Systems*. Addison-Wesley Publishing Company, Reading, MA.

Haftka, R., Martinovic, Z., Jr., W.H., and Schamel, G. (1986). An analytical and experimental study of a control system's sensitivity to structural modifications. *AIAA Journal*, 25, 310–315.

Hale, A., Lisowski, R., and Dahl, W. (1985). Optimal simultaneous structural and control design of maneuvering flexible spacecraft. *Journal of Guidance, Control, and Dynamics*, 8, 86–93.

Khot, N. and Abhyankar, N. (1993). Integrated optimum structural and control design. In M.P. Kamat (ed.), *Structural Optimization: Status and Promise*. Washington, D.C.

Lim, K. and Gawronski, W. (1993). Modal Grammian approach to actuator and sensor placement for flexible structures. *AIAA Journal*, 31, 674–684.

Muller, P.C. and Weber, H.I. (1972). Analysis and optimization of certain qualities of controllability and observability for linear dynamical systems. *Automatica*, 8, 237–246.

Oldham, K., Huang, X., Chahwan, A., and Horowitz, R. (2005). Design, fabrication and control of a high-aspect ratio microactuator for vibration suppression in a hard disk drive. In *Proceedings of the IFAC World Congress*. Prague.

Ouyang, P., Zhang, W., and Wu, F. (2002). Nonlinear PD control for trajectory tracking with consideration of the design for control methodology. In *Proceedings of the IEEE International Conference on Robotics & Automation*, 4126–4131. IEEE, Washington, D.C.

Park, J. and Asada, H. (1992). Integrated structure/control design of a two-link nonrigid robot arm for high speed positioning. In *Proceedings of the IEEE International Conference on Robotics & Automation*. IEEE, Nice, France.

Peters, D.L. (2010). *Coupling and Controllability in Optimal Design and Control*. PhD Thesis, University of Michigan, Ann Arbor, MI.

Peters, D.L., Kurabayashi, K., Papalambros, P.Y., and Ulsoy, A.G. (2008). Co-design of a MEMS actuator and its controller using frequency constraints. In *Proceedings of the ASME Dynamic Systems and Control Conferences*. ASME, Ann Arbor, MI. Paper number DSCC 2008-2212.

Peters, D.L., Papalambros, P.Y., and Ulsoy, A.G. (2009). On measures of coupling between the artifact and controller optimal design problems. In *Proceedings of the ASME Design Engineering Technical Conference & Computers in Engineering Conference*. ASME, San Diego, CA. Paper number DETC 2009-86868.

Peters, D.L., Papalambros, P.Y., and Ulsoy, A.G. (2010). Relationship between coupling and the controllability Grammian in co-design problems. In *Proceedings of the American Control Conference*. ASME, Baltimore, MD. (accepted).

Pomrehn, L. and Papalambros, P. (1994). Global and discrete constraint activity. *Journal of Mechanical Design*, 116, 745–748.

Rao, S. and Pan, T. (1990). Modeling, control, and design of flexible structures: A survey. *Applied Mechanics Review*, 43, 99–117.

Ravichandran, T., Wang, D., and Heppler, G. (2006). Simultaneous plant-controller design optimization of a two-link planar manipulator. *Mechatronics*, 16, 233–242.

Roh, H. and Park, Y. (1997). Actuator and exciter placement for flexible structures. *Journal of Guidance, Control, and Dynamics*, 20, 850–856.

Skogestad, S. and Postlethwaite, I. (2005). *Multivariable Feedback Control: Analysis and Design*. John Wiley and Sons, Ltd., West Sussex, UK.

Zhu, Y., Qiu, J., and Tani, J. (2001). Simultaneous optimization of a two-link flexible robot arm. *Journal of Robotic Systems*, 18, 29–38.